Quantal Sarcomere-Length Changes in Relaxed Single Myofibrils

Felix Blyakhman, Anna Tourovskaya, and Gerald H. Pollack
Department of Bioengineering, University of Washington, Seattle Washington 98195 USA

ABSTRACT We carried out experiments on single isolated myofibrils in which thin filaments had been functionally removed, leaving the connecting (titin) filaments as the sole agent taking up the length change. With technical advances that gave sub-nanometer detectability we examined the time course of single sarcomere-length change when the myofibril was ramp-released or ramp-stretched by a motor. The sarcomere-length change was stepwise. Step sizes followed a consistent pattern: the smallest was ~2.3 nm, and others were integer multiples of that value. The ~2.3-nm step quantum is the smallest consistent biomechanical event ever demonstrated. Although the length change must involve the connecting filament, the size of the quantum is an order of magnitude smaller than anticipated from folding of Ig- or fibronectin-like domains, implying either that folding occurs in sub-domain units or that other mechanisms are involved.

INTRODUCTION

Recent experiments from this laboratory have shown that shortening in single myofibrillar sarcomeres occurs in stepwise fashion (Yang et al., 1998; Blyakhman et al., 1999). The steps have been observed during active shortening as well as in unactivated myofibrils released to shorten by a motor.

Although the mechanism of active stepping remains to be settled, steps in unactivated specimens seem inevitably associated with connecting filaments, for it is only connecting filaments that change length in the unactivated state. The possibility that connecting filaments undergo stepwise length changes is supported by experiments on isolated titin molecules. Rief et al. (1997) and Tskhovrebova et al. (1997) have shown that titin molecules and titin constructs consisting of serial Ig domains undergo stepwise length changes, at least during stretch. In the experiments by Rief et al. (1997) the steps were 25–30 nm, whereas the Tskhovrebova et al. results showed variable step size ranging between ~5 and 25 nm. Thus, length steps in titin molecules can be observed, but step size remains to be settled.

Initial attempts to explore this phenomenon in single myofibrils yielded step sizes in the range seen by Tskhovrebova et al. (1997). Although the single molecule steps were obtained during lengthening whereas the myofibril steps were obtained during shortening, we suggested that the two phenomena were likely to be related because of their similarity (Yang et al., 1998; Blyakhman et al., 1999). This suggestion implied a high level of cooperativity among the many hundreds of parallel connecting filaments spanning the myofibrillar cross section; otherwise the steps in each filament would be out of phase with the steps in others and the overall shortening pattern would be smooth, not stepwise.

The current experiments were carried out at considerably higher detection sensitivity. They were also carried out under the rigor-stretch protocol, which effectively defunctionalizes thin filaments by dislodging their anchor points from the Z-line, leaving the connecting filaments as the sole agent taking up any imposed length change. The possibility of force sharing with the thin filament is thereby eliminated. The main objective was to determine, with this less ambiguous I-band structure, whether the quantal step-size paradigm demonstrated earlier would be preserved. We also wished to determine whether the higher resolution might confirm the implied ~2.3-nm quantum.

MATERIALS AND METHODS

Except for several notable differences described below, the methods were largely the same as those used in earlier studies by Yang et al. (1998) and Blyakhman et al. (1999).

Apparatus

The apparatus is schematized in Fig. 1. The specimen was held in an experimental chamber by a fixed glass needle at one end and the glass tip of a piezomotor at the other end. We imaged the myofibril with phase-contrast microscopy, magnifying the image with a 100× phase-contrast objective and projecting it onto a linear 1024-element photodiode array (Reticon, Santa Clara, CA). Images were also obtained on video for visual inspection.

Intensity-scan data are shown in Fig. 2. The top panel shows the image of a representative myofibril, and a scan is shown below. Scans were obtained every 50 ms for a period of 30–50 s during the stretch-release cycle. Intensity profile data were then acquired and converted to sarcomere length by custom software (below) written in LabView. The lower panel shows a gray-scale image of the time course of intensity profile changes in successive scans (upward). As the motor imposes a rapid stretch, the striations move rightward and then return slowly to their initial positions during the subsequent slow release.

Solutions

Solution compositions are shown in Table 1.

Received for publication 18 October 2000 and in final form 26 April 2001.

F. Blyakhman's current address: Department of Physics, Ural State University, Ekaterinburg, Russia.

Address reprint requests to Dr. Gerald H. Pollack, University of Washington, Department of Bioengineering, Box 357962, Seattle, WA 98195. Tel.: 206-685-1880; Fax: 206-685-3300; E-mail: ghp@u.washington.edu.

0006-3495/01/08/1093/08 $2.00

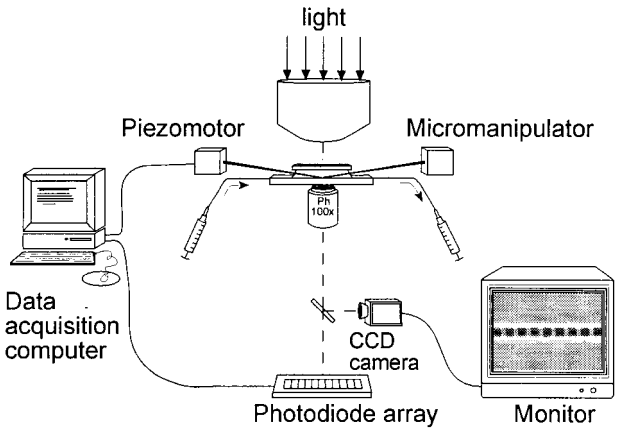

FIGURE 1 Schematic of apparatus.

Specimens

Single myofibrils from glycerinated bumblebee flight muscles were used. Bees were dissected at room temperature after immobilization by refrigeration. Two dorso-ventral flight muscles attached to the thorax were left in situ as the rest of the body was dissected away. Muscles were chemically skinned by soaking them alternately in solution A (1% (v/w) Triton X-100 in relaxing solution containing 10 μM leupeptin and 1 mM dithiothreitol) and solution B (50% glycerol in relaxing solution) at 4°C. Muscles were kept in solution B at −20°C for immediate use and at −80°C for longer-term storage. Myofibrils were isolated by using fine needles to disaggregate specimens on a cover glass in a drop of rigor solution. Striation patterns of varying quality were found, and we were careful to select only those specimens in which striations were clear, uniform, and apparently undisturbed.

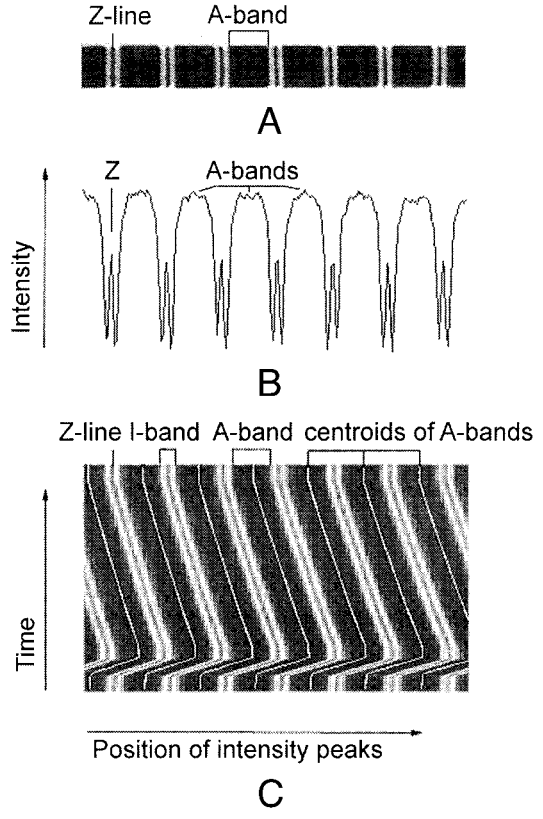

FIGURE 2 Analytical procedure used to measure the time course of single sarcomere-length change. (*A*) Phase-contrast image of representative myofibril; (*B*) Intensity trace along myofibril in *A*; (*C*) Gray-scale image of striations during motor-imposed length change. Centroid computation indicated.

TABLE 1 Solution composition

	K propionate (mM)	K_2EGTA (mM)	Mg acetate (mM)	Na_2ATP (mM)	NaN_3 (mM)	pH
Rigor	150	5	3		5	6.8
Relaxing	150	5	3	5	5	6.8

The myofibril of choice was then suspended between two glass needles in a chamber on the stage of the inverted (Zeiss Axiovert-35, Thornwood, NY) microscope. To mount the myofibril in the mechanical setup, each end was carefully wound around the tip of the respective glass needle by means of hydraulic micromanipulators. All manipulations were done in rigor solution.

Experiments were carried out on the rigor-stretch model (White and Thorson, 1973; Trombitás and Tigyi-Sebes, 1977), in which thin filaments are disengaged from the Z-line. This allowed us to focus solely on dynamics of the connecting filaments. To break thin filaments from their Z-line anchor points, the myofibril in rigor was quickly stretched and released several times in succession. Parallel thin filaments dislodge as a unit, migrating to the A-band in activating solution. The appearance of very bright I-bands indicated that breakage was achieved. Rigor solution was then exchanged to relaxing solution by injecting one solution from an inlet syringe while withdrawing the other with the outlet syringe (see Fig. 1). The solution was replaced every 30 min to ensure consistency of composition. We placed a small coverslip on the surface of the solution to avoid image distortions caused by surface unevenness.

Experimental protocols

The basic protocol was to impose ramp shortening or lengthening on the myofibril and measure the resultant sarcomere length changes. Generally, the overall length change was trapezoidal (Fig. 2). Motor-ramp speeds were selected to give two nominal speeds of sarcomere-length change: ~1 nm/s and ~8 nm/s. Because the exact speed of sarcomere-length change depended on the number of sarcomeres in the specimen and on the uniformity of the imposed length change, appreciable speed variation resulted (range, 0.5 to 3 nm/s and 5.5–10 nm/s). In some cases the motor was also used to impose stepwise length changes.

Sarcomere-length computation

To compute sarcomere length, we developed a new peak-detection algorithm (S. Sokolov, A. Grinko, A. Tourovskaia, F. Reitz, G. H. Pollack, and F. A. Blyakhman, submitted for publication) based on the minimum average risk method proposed by Kolmogorov (1931) and further implemented for signal processing in various fields (Duda and Hart, 1973; Huber, 1964; Martin and Schwarz, 1971).

The minimum-average-risk algorithm operates on repeated scans of an intensity peak, precisely quantifying peak movement between scans. This method is differential; it compares the respective A-band intensity peak with that of the one immediately previous. The algorithm is implemented by finding the optimal position of a scan relative to the first derivative of the immediately previous scan. Optimal registration occurs when the integrated pointwise product of these functions is minimized. From this, the peak shift from one scan to the next can be precisely quantified.

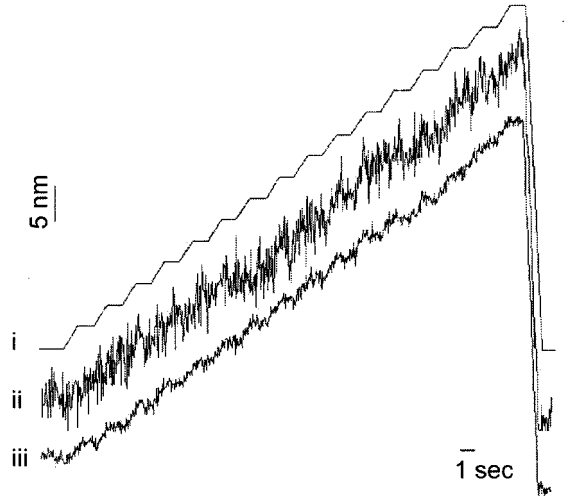

FIGURE 3 Comparative resolution of center of mass and minimum average risk algorithms. Trace i shows motor-command signal. Trace ii shows sarcomere length computed with the center of mass algorithm, whereas trace iii shows the same data analyzed with the minimum average risk method.

As implemented, a two-sarcomere-wide subsection of each successive digitized scan of a myofibril is selected to bracket a given A-band. The shift, relative to the derivative of the previous scan, required to obtain the best fit is determined. From the relative shift between two A-bands, the change of sarcomere length can be computed. By repeating this computation for each successive scan, the time course of each A-band position, and thus of sarcomere length, can be obtained. The resulting calculated positions of each A-band along the myofibril are shown in Fig. 2 *c* as the vertically oriented white lines running along the A-bands. From these traces, sarcomere lengths are computed automatically.

This method results in superior precision and yields a higher signal-to-noise ratio compared with the center-of-mass algorithm, which computes A-band intensity-peak medians as described in Yang et al. (1998). Comparison of the two methods is shown in Fig. 3. A stepwise stretch was imposed on the myofibril (*trace i*), and the sarcomere-length change was measured using both the center of mass algorithm (*trace ii*) and the minimum-average-risk algorithm (*trace iii*). Although sarcomeres are anticipated to follow the imposed pattern at least roughly, this pattern is only marginally discernible in *trace ii* because of noise. In *trace iii* root mean square noise is reduced to 1 nm or less and the imposed pattern is faithfully followed. Hence, the newer algorithm is some four to five times superior in noise reduction and step detectability.

Analysis

To analyze steps in sarcomere-length traces we used two different approaches. The first approach was to identify pauses by eye. Start and end points of each pause are noted, and an algorithm computes the best-fit line. Step size is then computed as the vertical decrement between centers of two successive pauses, as described in Yang et al. (1998). Step-size distribution is obtained by plotting all measured step sizes as histograms.

As an alternative approach we implemented the method proposed by Svoboda et al. (1993) for statistical analysis of kinesin stepping. For each sarcomere-length-change trace, we computed a periodogram, a histogram of time dwelled at each sarcomere length. Step plateaus appear in the periodogram as peaks at certain positions. The autocorrelation of the periodogram is then computed; any periodicity of the stepping is revealed as a peak at each recurrence of the frequency (or frequencies) of the periodicities. The power spectrum of this peak distribution yields the prevalence of each step size. These spectra may then be averaged to improve the signal-to-noise ratio. As shown by Svoboda et al. (1993) this approach has the capacity to clearly discern spatial frequencies corresponding to periodic step-like motion even from traces of modest signal-to-noise ratio.

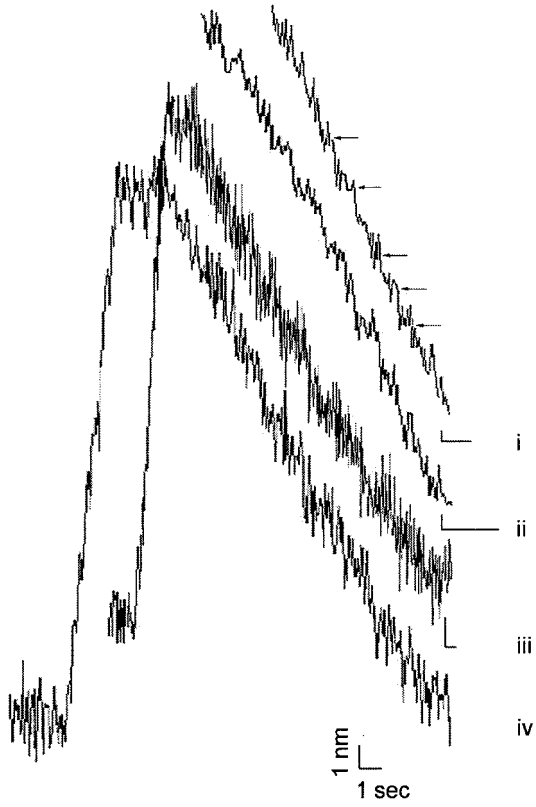

FIGURE 4 Representative traces of single sarcomere length versus time. Upper records show segments of more extended traces. Lower records show full traces of rapid stretch-hold-slow release. Arrows on upper trace denote prominent pauses. Calibration factors, 1 nm and 1 s, apply throughout.

RESULTS

Fig. 4 shows four representative traces of sarcomere length versus time. In these experiments the myofibril was rapidly stretched, held, and then subjected to a smooth ramp release. Sarcomere-shortening traces contain multiple pause periods (arrows). During these periods the sarcomere-length change was indistinguishable from zero. Between pauses, the sarcomere shortened in steps of several nanometers. Although larger steps are occasionally discernible, steps are generally much smaller than those reported earlier (Yang et al., 1998; Blyakhman et al., 1999). Mainly, this is because of the increase of signal-to-noise, which allowed short pauses previously buried in the noise to emerge more distinctly. Also, striations had higher contrast because the rigor-stretch pro-

tocol removes thin filaments from the I-band. Thus, steps of smaller size were readily detectable.

The average number of steps per shortening trace of nominally 20–30 nm was 5.4 ± 1.8 (n = 37 traces). The fraction of time taken up by distinct steps and pauses was 38.3 ± 13.4%, the remaining time containing no features discernible beyond the noise. Such relative fractions, however, are criterion dependent. To define a pause, the criterion used here was that the slope of the line that best fit at least five consecutive sample points had to be close (cf. Blyakhman et al., 1999) to zero. If, say, a more liberal, three-successive-data-point minimum instead of five had been considered, the fraction occupied by steps and pauses would have exceeded 38%. At any rate, steps and pauses accounted for an appreciable fraction of each trace.

Controls for potential artifact in these procedures have been described (Yang et al., 1998; Blyakhman et al., 1999). Several potential artifacts were examined. The effects of discreteness of the photodiode array were checked by using two magnifications and also by substituting a nondiscrete sensor for the discrete photodiode array. Although 2.7-nm steps did not lie within the realm of detectability in any of these approaches, the discernible, larger steps were essentially similar with all methods. Specimen-translation artifacts were checked by demonstrating that smoothly translating A-bands showed no steps. The method was capable of detecting any of the larger steps reported here (e.g., 6.7 nm) if they had been present, but no such steps were found. (A similar, updated control is implicit in Fig. 5, below, where high-resolution records of A-band translation (*trace ii*) show no spontaneous discernible steps). Finally, algorithm-based uncertainties were checked by demonstrating that at least for the larger steps, similar step distributions could be obtained using two different algorithm implementations (Yang et al., 1998; Blyakhman et al., 1999). Thus, all tests have proved negative for artifact. In the current experiments we add an additional control to test for the ability to obtain sub-nanometer precision.

For this control, the motor imposed a linked series of sarcomere-shortening steps of nominally ~2.7 nm, slightly different from the anticipated step size (see below). In Fig. 5 the top trace shows the motor-command signal. Motor position is approximated by the second trace. The trace shows the position of an A-band situated close to the motor, which served as an approximate marker of motor position. (For technical reasons motor position itself could not be measured with sufficiently high resolution.) The next trace shows a representative sarcomere-shortening record. Note the prominent appearance of the 2.7-nm steps, which follow the motor-imposed pattern quite closely, similar to Fig. 3. Some traces, however, show intervening short pauses (*trace iv*, *arrows*), implying steps of smaller size generated spontaneously. Note that the spontaneous pauses tend to cluster near the motor-imposed pauses.

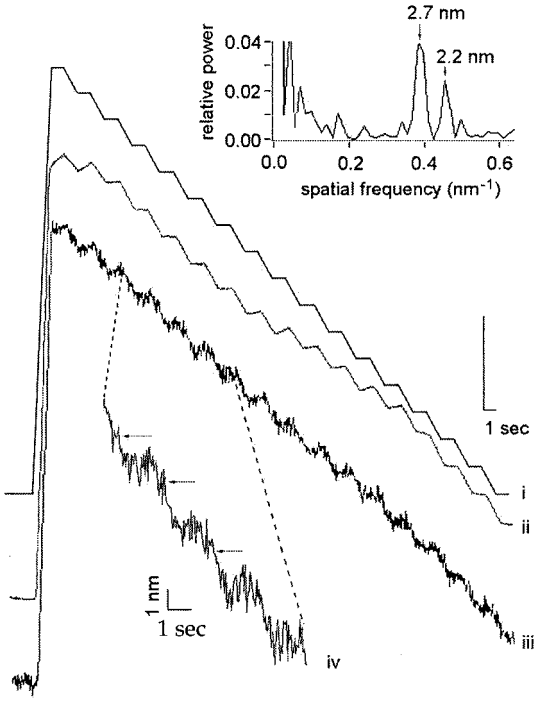

FIGURE 5 Analysis of motor-imposed and spontaneous steps. (*Top trace*) Command signal to motor; (*second trace*) motor movement assessed through translation of an A-band close to motor; (*third trace*) sarcomere length versus time; (*bottom trace*) magnified view of third trace. Scales, 290 nm (*second trace*); 10 nm (*third trace*). (*Inset*) Corresponding sarcomere-shortening power spectra.

Step-size distribution was analyzed using the power-spectrum method, and the result is shown in the inset. The peak at 2.7 nm corresponds to the motor-imposed step. This is expected. The secondary peak at 2.2 nm corresponds to the spontaneously generated steps. In terms of size, the 2.2-nm value is indistinguishable from the 2.3-nm value observed during various motor-imposed ramps (see Figs. 6, 7, 9, and 10). The fact that the two sizes, 2.2 and 2.7 nm, could be resolved in the same set of traces implies that signal quality is sufficient to achieve a resolution of <0.5 nm, or several angstroms.

A second control was run to test for the effects of noise. We acquired a long baseline sarcomere-length versus time signal, which contained noise. A linear ramp was added to this signal to simulate step-free shortening. This summed signal was compared with the actual sarcomere shortening that took place (at similar speed) just after the baseline period. Power-spectrum analyses of the respective signals are shown in Fig. 6. The real sarcomere shortening trace, Fig. 6 *a*, shows the anticipated peak at 2.3 nm as well as a peak at twice that value. The simulated shortening trace, Fig. 6 *b*, shows only noise, with nothing of significance at 2.3 nm. Thus, the peaks seen in the above histograms or power spectra did not arise from noise.

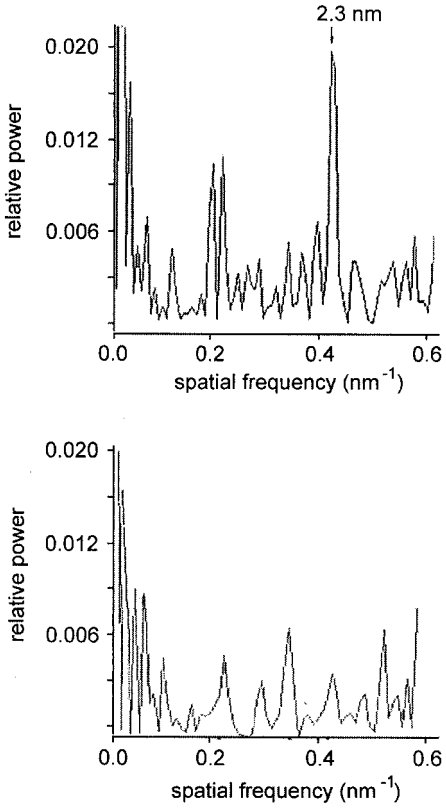

FIGURE 6 Power spectra measured from a sarcomere-shortening record (*a*), and from a record consisting of baseline (no shortening) plus a computer-generated ramp (*b*). The latter shows only noise, whereas the former shows steps at 2.3 nm. In repeats with nine sarcomere-length traces from the same myofibril, peaks with mean amplitude 0.011 ± 0.0043 SD always fell between 2.2 and 2.3 nm (bin width 0.5 nm).

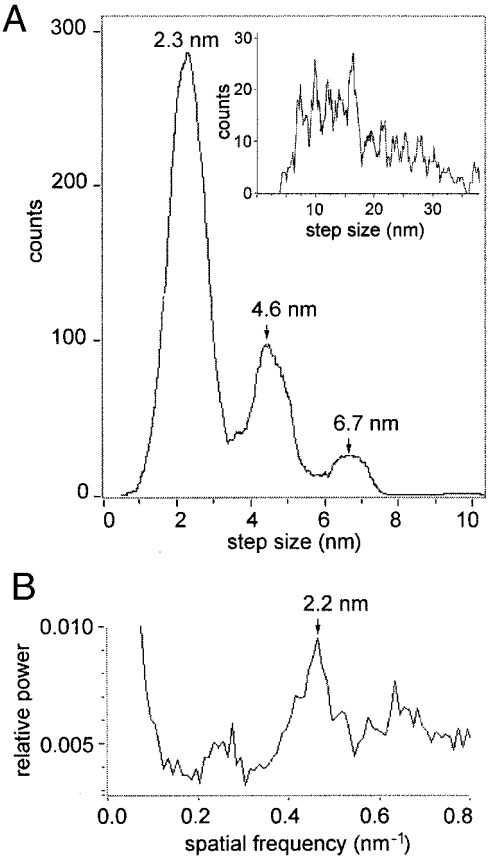

FIGURE 7 Distribution of shortening-step size. (*a*) Histogram of step size obtained from 514 shortening steps from 11 myofibrils. Arrows denote peak locations. Inset shows earlier data from Blyakhman et al. (1999) obtained with lower signal-to-noise ratio. (*b*) Same data as in *a*, analyzed in terms of relative power at different spatial frequencies.

Having established that the signal has the requisite sensitivity and noise immunity, we proceeded to analyze step sizes. Results obtained for imposed shortening ramps are shown in Fig. 7. In Fig. 7 *a*, sizes were computed using an algorithm that determined the vertical decrement between successive pauses (Yang et al., 1998). The main peak is centered at ~2.3 nm. Secondary peaks are centered at 4.6 nm and ~6.7 nm, approximately two and three times the spacing of the main peak. These plots contain data from low- and higher-speed releases; in lower-speed releases the center of gravity fell more heavily toward the left relative to higher-speed releases, but there were no obvious differences of peak locations (not true of stretch; see below). The inset shows earlier results obtained at lower resolution (Blyakhman et al., 1999). Peaks are spaced at ~2.3-nm intervals as well, but because of limited resolution the smallest multiples are missed. Data sets are otherwise complementary.

In Fig. 7 *b*, the data of Fig. 7 *a* are analyzed by the power-spectrum method, which is based on the frequency content of the dwell time at each sarcomere length (Svoboda et al., 1993; Block and Svoboda, 1995). The method is distinct from the one used in Fig. 7 *a*. Results show a ~2.2-nm peak as well as a higher-order peak at about twice that value. Thus, the two analytical procedures give essentially the same result.

Effects of stretch are examined in Figs. 8-10. Fig. 8 shows representative sarcomere-length traces obtained during stepwise (*traces i* and *ii*) and ramp (*trace iii*) stretches. Pauses are detectable during the imposed ramp (*trace iii*, *arrows*) but somewhat less distinctly than those seen during shortening (Fig. 4). In *traces i* and *ii*, imposed steps were nominally 18 nm and are faithfully reproduced in the sarcomere-length traces. These traces also show spontaneous pauses (*arrows*) similar to those seen in Fig. 5.

Spontaneous pauses were analyzed and plotted in Fig. 9. Two peaks are seen. The broad peak at the right reflects the imposed forcing function, with a peak at ~18 nm. The narrower peak at the left reflects steps arising from the spontaneously generated pauses. These steps occur at 2.30 nm. Hence the stretch quantum is the same size as the shortening quantum.

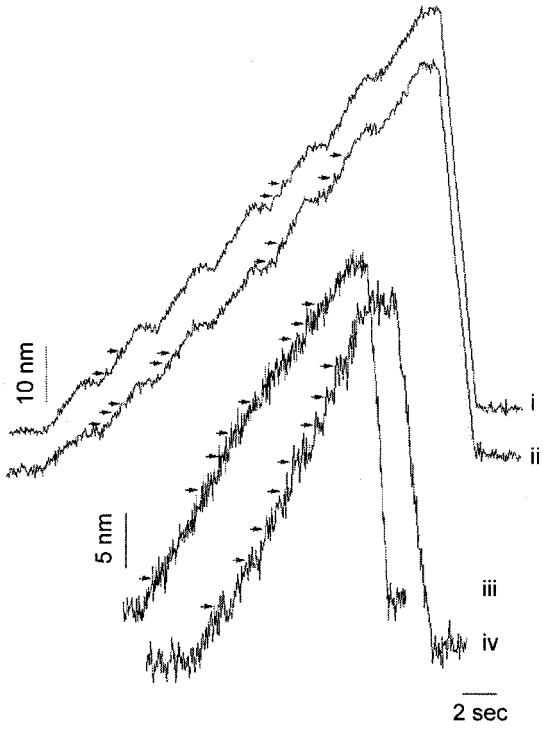

FIGURE 8 Time course of sarcomere-length increase measured during staircase (*i* and *ii*) and ramp (*iii* and *iv*) length changes. In traces *i* and *ii*, arrows indicate spontaneous pauses that occur between the longer pauses corresponding to those imposed by the motor. In traces *iii* and *iv*, arrows denote discernible pauses.

Fig. 10 analyzes step size obtained during applied stretching ramps. For the lower speed, the peak is once again at 2.30 nm. The power-spectrum method gives a comparable value of 2.38 nm. For the higher-speed stretches, multiple histogram peaks were obtained. These peaks fell at ~2.5 nm, ~5.0 nm, and ~7.5 nm, although exact peak locations

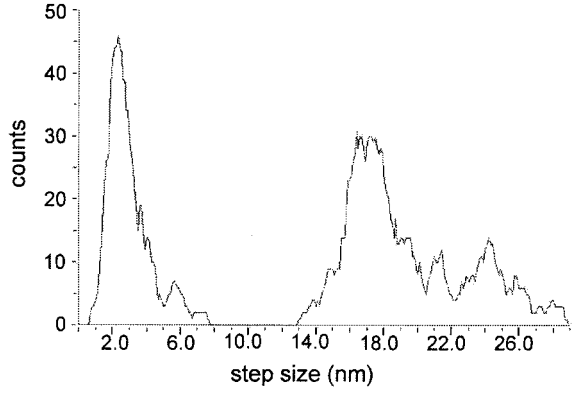

FIGURE 9 Histogram of step sizes obtained during staircase-like stretch. Steps corresponding to staircase treads occur at ~18 nm (broad peak at right), whereas the narrower peak at 2.30 nm reflects spontaneous events. Histogram includes 264 steps.

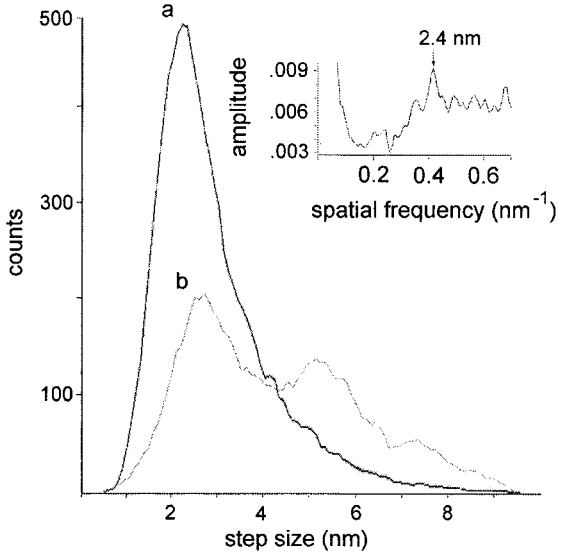

FIGURE 10 Histogram of step size obtained during stretching ramp. (*a*) Low speed (1012 steps); (*b*) High speed (759 steps). Inset shows step size computed using the power-spectrum method.

were uncertain because the peaks were broad. This resulted in part from the relative shortness of pauses (the power-spectrum method was unable to discern the primary peak). Thus, the shift from 2.3 nm to 2.5 nm is somewhat uncertain and awaits future improvements in resolution for confirmation.

DISCUSSION

The results show that the fundamental shortening quantum in the unactivated state is ~2.3 nm. In this state, and particularly in the current experiments where the thin filament is functionally eliminated, the sole element mediating shortening is the connecting (titin) filament. Hence, the steps must somehow reflect connecting-filament dynamics. Previous myofibril experiments with similar protocols have shown that stepping behavior in complementary half-sarcomeres is asynchronous (Blyakhman et al., 1999). Thus, the 2.3-nm step is a reflection of the dynamics of one of the sarcomere's two sets of connecting filaments.

A second result of significance is that the size of the quantum is the same for release and for stretch. The 2.3-nm quantum was extremely robust for shortening, independent of whether the imposed forcing function was step-like or ramp-like. In the case of stretch, the 2.3-nm value was also robust except for the single case of high velocity stretch. One possibility is that the high forces associated with rapid stretch result in slight elongation of certain structures of otherwise constant length, yielding the slightly higher step sizes. Alternatively, because of relatively short pauses, the apparent difference may arise from experimental error. Except for this issue, step size during

stretch was identical to that during release. Both were integer multiples of 2.3 nm.

The idea that connecting filaments might change length in steps is implicit in molecular studies. In both highly loaded single titin molecules and titin constructs consisting of a string of Ig-like domains, Rief et al. (1997) found that linear stretch ramps produced sawtooth-tension waveforms. This was interpreted to imply discrete Ig-domain unfoldings. Similarly in single isolated titin molecules, Tskhovrebova et al. (1997) induced rapid stretch and observed that the subsequent tension decay was stepwise. In the former study, step size was 25–28 nm, and in the latter, most steps were in the range of 5–20 nm. The source of the difference is unclear, although a force difference may be responsible; nor is it clear whether steps smaller than 5 nm might have been observable with higher resolution.

Because titin molecules can manifest stepwise length changes, it is tempting to attribute the steps observed here to steps in titin. If the shortening steps are associated with the folding of the connecting filament's Ig or fibronectin-III domains, then such domains apparently fold in stages, for the step produced by a domain's fold-unfold transition is an order of magnitude larger than 2.3 nm found here (Rief et al., 1997). The Ig domain for example contains ~90 residues and has a sevenfold antiparallel β-barrel structure (Erickson, 1994; Improta et al., 1996). Each turn of the β structure should therefore be several nanometers in length. The 2.3-nm step could then imply folding one turn at a time, each fold accounting for the quantal step. Sub-domain unfolding is not without precedent; it appears also to occur in albumin (Zocchi, 1997). Thus, connecting-filament domains could conceivably fold or unfold in stages, each event producing a 2.3-nm step.

However, this hypothesis carries several areas of concern. First, the regularity of the steps seen here implies a structural basis more regular than might be expected from the folding patterns of the respective β-sheet domains. Second, steps in single titin molecules are observed during stretch only, whereas our results have shown steps during both stretch and release. Finally, as mentioned above, the explanation demands unfolding of sub-domains, not entire domains. Thus, a connecting-filament step arising from titin-domain dynamics is by no means certain.

An alternative possibility is that the steps might arise from another element lying within the connecting filament. In addition to titin or titin-like proteins, there is some evidence that the connecting filament may also contain tropomyosin, running axially, along with titin (for review, see Pollack, 1990). Tropomyosin is an α-helical coiled-coil much like the myosin rod. Positive charges repeat axially at 6.5 to 7 times per 100 residues (Katayama and Nonomura, 1979). With the axial residue advance of 1.49 Å characteristic of the α-helix, this translates to a regular charge repeat along the molecule at every ~2.2 nm along the molecule. Thus, tropomyosin molecules sliding over one another, driven by the retractive force of titin, could give the observed ~2.3-nm periodicity.

Such an explanation fits within the realm of the so-called stick-slip mechanism. When closely spaced parallel surfaces with intervening fluid are induced to shear past one another, translation occurs in steps punctuated by pauses (Israelachvili et al., 1990; Yoshizawa and Israelachvili, 1993; Bhushan et al., 1995). This shear phenomenon is thus similar to the one observed here, and the stick points could arise from opposite charges on adjoining tropomyosin molecules.

Whatever may be the molecular source of the steps, an implication is high cooperativity among parallel elements, for if parallel connecting filaments did not step synchronously the sarcomere would show smooth shortening. One possible mediator of synchrony may be the radial cross-links between I-band filaments. These links are seen clearly in thin electron microscope sections and also in specimens prepared by freeze-fracture (Trombitás et al., 1988; Pollack, 1990). If sufficiently stiff, they could constrain parallel filaments to act in unison, so that a step in one filament could not take place without a similar step in a neighboring filament.

Another potential mediator is water. Water is tightly held in the myofibrillar lattice, and there is evidence that such tenacity may be explained by strong water adsorption to filaments (Ling, 1984; Clegg, 1984; Wiggins, 1990; Pollack, 2001). In this line of thinking, water is largely organized around protein filaments, practically as a solid. Any change of water induced by a local change in one filament would thus be felt by the corresponding region in parallel filaments. Hence, the ensemble would change length synchronously.

Although these results do not definitively pinpoint the source of the steps, they confirm the earlier hypothesis that shortening is quantal. Histograms had implied that step size might be an integer multiple of ~2.3 nm (Fig. 7, *inset*), but it was not clear whether the histogram peaks' uniform spacing was a coincidental feature or whether indeed it represented multiples of an ~2.3-nm quantum. Figs. 7, 9, and 10 demonstrate that the quantum exists, both for shortening and stretch. Fig. 7 also shows the $n = 2$ and $n = 3$ multiples of this quantum, the latter apparent in the older data (Yang et al., 1998; Blyakhman et al., 1999).

Finally, it is of interest that the consistent step size seen here may be the smallest observed to date in any biological system. Whether still smaller steps may be observable as resolution continually improves remains to be seen.

REFERENCES

Bartoo, M. L., V. I. Popov, L. Fearn, and G. H. Pollack. 1993. Active tension generation in isolated skeletal myofibrils. *J. Muscle Res. Cell Motil.* 14:498–510.

Bhushan, B., J. Israelachvili, and U. Landman. 1995. Nanotribology: friction, wear and lubrication at the atomic scale. *Nature.* 374:607–616.

Block, S. M., and K. Svoboda. 1995. Analysis of high resolution recordings of motor movement. *Biophys. J.* 68:230s–241s.

Blyakhman, F., T. Shklyar, and G. H. Pollack. 1999. Quantal length changes in single contracting sarcomeres. *J. Muscle Res. Cell Motil.* 20:529–538.

Clegg, J. S. 1984.. Intracellular water and the cytomatrix: some methods of study and current views. *J. Cell Biol.* 99:167s–171s.

Duda, R. O., and P. E. Hart. 1973. Pattern Recognition and Scene Analysis. John Wiley and Sons, New York.

Erickson, H. P. 1994. Reversible unfolding of fibronectin type III and immunoglobuilin domains provides the structural basis for stretch and elasticity of titin and fibronectin. *Proc. Natl. Acad. Sci. U.S.A.* 91: 10114–10118.

Huber, P. J. 1964. Robust estimation of a location parameter. *Ann. Math. Stat.* 35:73–104.

Improta, S., A. S. Politou, and A. Pastore. 1996. Immunoglobulin-like modules from titin I-band: extensible components of muscle elasticity. *Structure.* 4:323–337.

Israelachvili, J., P. McGuiggan, M. Gee, A. Homola, M. Robbins, and P. Thompson. 1990. Liquid dynamics in molecularly thin films. *J. Phys. Condens. Matter.* 2:SA89–SA98.

Katayama, E., and Y. Nonomura. 1979. Electron microscopic analysis of tropomyosin paracrystals. *J. Biochem.* 86:1511–1522.

Kolmogorov, A. 1931. Uber die analytischen Methoden in der Wahrscheinlichkeitsrechnung. *Math. Ann.* 104:415–458.

Ling, G. L. 1984. In Search of the Physical Basis of Life. Plenum, New York.

Martin, R. D., and S. C. Schwarz. 1971. Robust detection of a known signal in nearly Gaussian noise. *IEEE Trans.*17:50–55.

Pollack, G. H. 1990. Muscles and Molecules: Uncovering the Principles of Biological Motion. Ebner and Sons, Seattle.

Pollack, G. H. 2001. Cells, Gels and The Engines of Life. Ebner and Sons, Seattle.

Rief, M., M. Gautel, F. Oesterhelt, J. M. Fernandez, and H. E. Gaub. 1997. Reversible unfolding of individual titin immunoglobulin domains by AFM. *Science.* 276:1109–1112.

Svoboda, K., C. F. Schmidt, B. J. Schnapp, and S. M. Block. 1993. Direct observation of kinesin stepping by optical trapping interferometry. *Nature.* 365:721–727.

Trombitás, K., and A. Tigyi-Sebes. 1977. Fine structure and mechanical properties of insect muscle. *In* Insect Flight Muscle. R. T. Tregear, editor. North Holland Publishing, Amsterdam. 79–90.

Trombitás, K., P. H. W. W. Baaatsen, and G. H. Pollack. 1988. I-bands of striated muscle contain lateral struts. *J. Ultrastructure Mol. Struct. Res.* 100:13–30.

Tskhovrebova, L., J. Trinick, J. A. Sleep, and R. M. Simmons. 1997. Elasticity and unfolding of single molecules of the giant muscle protein titin. *Nature.* 387:308–312.

White, D. C. S., and J. Thorson. 1973. The kinetics of muscle contraction. *Prog. Biophys. Mol. Biol.* 27:173–255.

Wiggins, P. M. 1990. Role of water in some biological processes. *Microbiol. Rev.* 54:432–449.

Yang, P., T. Tameyasu, and G. H. Pollack. 1998. Stepwise dynamics of connecting filaments measured in single myofibrillar sarcomeres. *Biophys. J.* 74:1473–1483.

Yoshizawa, H., and J. Israelachvili. 1993. Fundamental mechanisms of interfacial friction. II. Stick-slip friction of spherical and chain molecules. *J. Phys. Chem.* 97:11300–11313.

Zocchi, G. 1997. Proteins unfold in steps. *Proc. Natl. Acad. Sci. U.S.A.* 94:10647–10651.